J. Plasma Fusion Res. SERIES, Vol. 5 (2002) 333–336

70 GHz Electron Cyclotron Resonance Heating System for Heliotron J

SHIDARA Hiroyuki, NAGASAKI Kazunobu[1], SAKAMOTO Kinzo[1], YUKIMOTO Hidetoshi, NAKASUGA Masahiko, SANO Fumimichi[1], KONDO Katsumi, MIZUUCHI Tohru[1], OKADA Hiroyuki[1], BESSHOU Sakae, MANABE Yoshito, ANG Wan Leng, KAWAZOME Hayato, MAENO Shogo, TAKEDA Masafumi, TAKAMIYA Tasho, TOMIYAMA Keishi, TSURU Hiroki, OHNO Yoshinori, KUBO Hiroyasu, NISHIOKA Yusuke, IRIGUCHI Masao, ORLOV Victor[2], PAVELYEV Alexander[2], TOLKACHEV Alexander[2], TRIBALDOS Victor[3] and OBIKI Tokuhiro[1]

Graduate School of Energy Science, Kyoto University, Uji 611-0011, Japan
[1] Institute of Advanced Energy, Kyoto University, Uji 611-0011, Japan
[2] GYCOM, Ulyanov Street, 603600 Nizhny Novgorod, Russia
[3] Asociacion Euratom-Ciemat para Fusion, Madrid 28040, Spain

(Received: 11 December 2001 / Accepted: 4 June 2002)

Abstract

A 70 GHz electron cyclotron resonance heating (ECRH) system has been constructed in Heliotron J, a helical-axis heliotron device, in order to realize localized heating and current drive experiments. This ECRH system consists of a gyrotron, a matching optics unit (MOU), a waveguide transmission line with the HE_{11} mode, polarizers, a barrier window and a launching system. The low power transmission test shows that the beam radius of the focused Gaussian beam is 22 mm at the magnetic axis, which is small enough compared to the averaged minor plasma radius (170 mm), and the launching system covers a wide steering range which is necessary for controlling the power localization in the three-dimensional helical-axis configuration. In the high power transmission test, the transmission efficiency of the corrugated waveguide of 20 m in length is 92 %, and the available output power to the vacuum vessel is up to 0.4 MW.

Keywords:

ECH, Heliotron J, localized heating, current drive, Gaussian beam, transmission efficiency

1. Introduction

ECRH has widely been used in many magnetic confinement devices. Especially in helical coil devices, the current-free plasma is routinely produced by this heating method. The helical-heliotron plasma device, Heliotron J, has begun its experiment since December 1999, and a 53.2 GHz ECRH system has been used for plasma production and heating [1]. Since the 53.2 GHz system has the injected power of TE_{02} axisymmetric mode, the power absorption was not localized, and the low single pass absorption caused a low heating efficiency. We introduced a new 70 GHz ECRH system for the purpose of localized heating, which makes it possible to perform various experiments such as plasma profile control and electron cyclotron current drive. The

Corresponding author's e-mail: shidara@center.iae.kyoto-u.ac.jp

Heliotron J device has three-dimensional magnetic field structure and spatial magnetic axis. Due to its complex shape, a wide range of injection angle and polarization with precise control is required to achieve the efficient single pass absorption. The 70 GHz ECRH system is designed and constructed to satisfy these requirements. In this paper, we report the overview of the 70 GHz ECRH system and the results of the low and high power transmission tests.

2. 70 GHz ECRH System

We have designed the ECRH system for the second harmonic of the extraordinary (X-) mode at the resonant magnetic field of 1.25 T. The system consists of the following components: a gyrotron, a MOU, a transmission line, a Boron Nitride barrier window and a launching system as shown in Fig. 1. The gyrotron manufactured by GYCOM has the operational frequency of 70.0 GHz, the maximum power of 600 kW at the output window, the pulse duration up to 500 ms and the Gaussian beam output mode. The output beam irradiated from the gyrotron window, which has an elliptic Gaussian shape with the linear polarization, is put into the MOU for correcting the beam shape to a circular one. The MOU has two phase correcting mirrors and water-flowing pipe for absorbing spurious modes and diffracted waves. The corrected Gaussian beam is coupled to the HE_{11} waveguides mode. The transmission line is composed of corrugated waveguides of totally 20 m long and 63.5 mm diameter, and three miter bends. Two grooved plane mirrors are assembled in the bends for adjusting the beam polarization. One is designed as a linear polarizer which can rotate the polarization plane, and the other is designed as a circular one which can control the ellipticity. The transmission line can be evacuated to avoid arc breakdown. The transmitted beam is injected into the Heliotron J plasma by the launching system as shown in Fig. 2. The launcher has two mirrors, a focusing ellipsoidal mirror [2] and a steering plane mirror. The focusing mirror focuses the beam of which the waist is located at the magnetic axis in the perpendicular injection case. The steering mirror can control the beam direction both toroidally and poloidally.

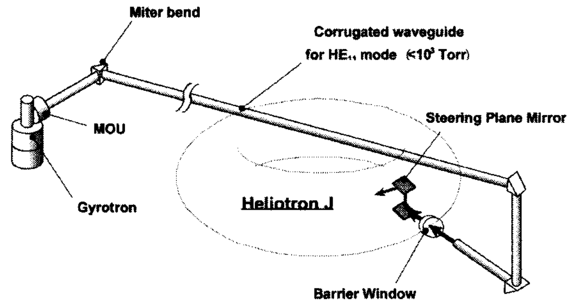

Fig. 1 Schematic view of the 70 GHz ECRH system in Heliotron J.

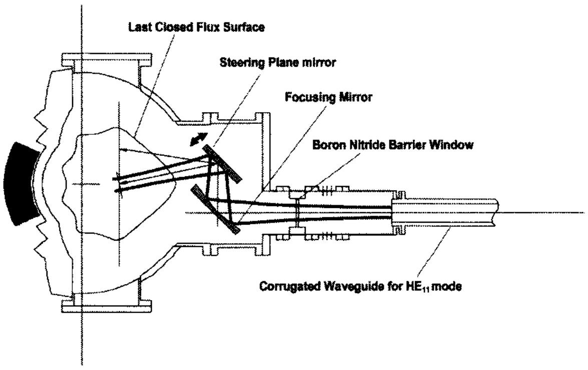

Fig. 2 Poloidal cross section of launching system.

3. Performance Results

3.1 Low power test

The performance of the polarizers and the launching system has been examined in a low power condition. The TE_{10} rectangular output mode from a 70 ($\pm$0.2) GHz, 20 mW output Gunn oscillator is converted into the HE_{11} mode using a waveguide mode converter. The purity of the HE_{11} mode is 97 % for this low power beam. We set a polarizer in a miter bend by replacing the reflecting plane mirror. We can change the polarization by rotating the polarizer. The miter bend is connected to 1-m waveguides for both sides. The beam shape and the polarization mode are measured with a diode detector in free space to suppress the effect of standing waves.

Figure 3 shows the results for the linear and circular polarizers. The definition of the rotation angle, α, and the ellipticity, β, is the same as in ref. [3]. The theoretical curves are also plotted, which are given by using integral method developed in the vector theories of diffraction gratings [3]. According to the calculation, the sinusoidally grooved mirror of the deep depth, $d/\lambda=0.50$, can rotate the polarization arbitrary with small ellipticity in the range of the polarizer rotation angle, $60° \le \phi \le 115°$, and the mirror of the shallow depth, $d/\lambda=0.30$, makes almost circular polarization at $\phi=55°$ and 125°. Here d and λ are the grooved depth

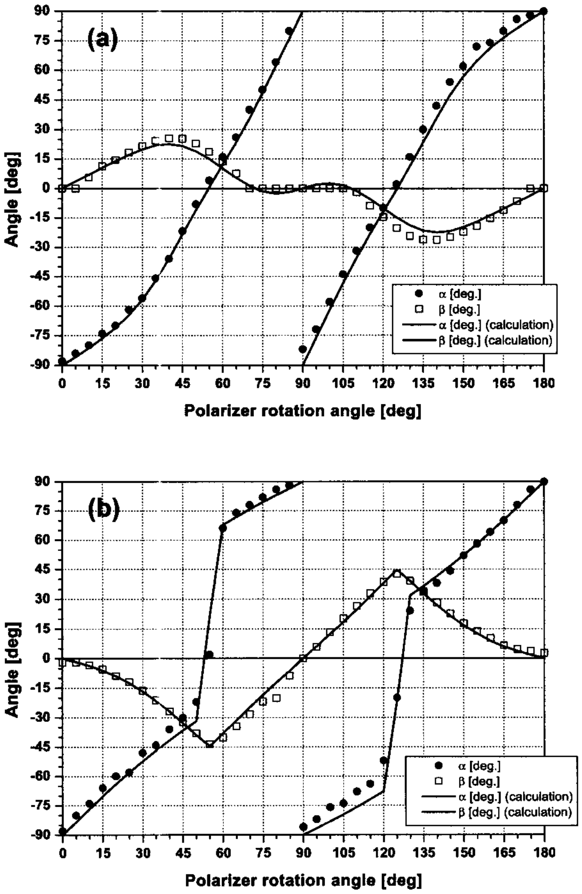

Fig. 3 Results of polarization measurement; (a) linear polarizer and (b) circular polarizer.

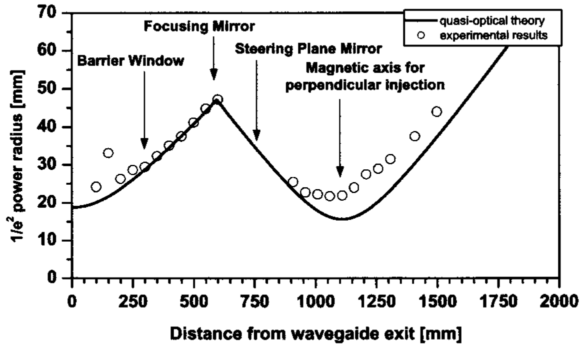

Fig. 4 Beam radius, as a function of the distance from the waveguide exit in the low power measurement.

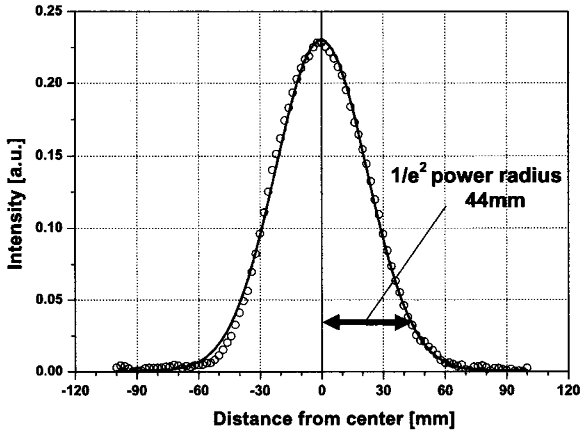

Fig. 5 Beam distribution in vertical direction at 390 mm after the focal point in the low power measurement.

and the wavelength, respectively. Since the experimental results are in a good agreement with the theoretical values for each polarizer, we conclude that the grooved mirrors are manufactured as designed. It is possible to control the rotation and the ellipticity independently, by combining these two polarizers.

The launching system is also tested in the same low power measurement system. We use a three-axis measuring system, which can measure the beam distribution and polarization plane for estimating the $1/e^2$ power radius from the radiation pattern. The size of the focusing mirror is 215×140 mm^2, and the steering plane mirror is 157×86 mm^2, which are 1.5 times larger than the beam diameter. The mirrors of this size can cover over 98 % of the power. Figure 4 shows the dependence of the beam radius as a function of the distance from the waveguide exit. The solid line gives the value derived from a quasi-optical theory, where the spot size of the beam is assumed 18.8 mm at the waveguide exit [4,5]. The spatial resolution is determined by the waveguide size of the detector. A rectangular waveguide of W band (2.54×1.27 mm^2) is used to detect the beam radiation. The measurement results shows that the Gaussian beam is focused and the beam radius is 22 mm at the major axis for perpendicular injection, although the beam radius is a little larger than the theoretical value. The beam shape is kept circular Gaussian after the focal point. The expected power density, which is defined by the power divided by the $1/e^2$ folding area at the focal point, is as high as 26 kW/cm^2. Figure 5 shows an example of beam shape after the focal point. After passing the focal point, the beam diverges as expected and the shape is kept Gaussian.

The direction range of the launching beam has been measured with a laser pointer (diameter 3 mm) at first set on the beam axis. Then we have confirmed the beam direction at several points using the low power millimeter wave oscillator. The steering range is ±15° and ±23° in toroidal and poloidal directions, respectively. These ranges are limited by the mechanical restriction of the mirror system in the launcher. The toroidal range corresponds to the angle from 60° to 120° between incident beam wave number and the magnetic field direction, and the poloidal range corresponds to $0 \leq r/a \leq 0.7$, where r is the averaged plasma minor radius and a is the averaged radius of the last closed flux surface. This poloidal range is sufficient for controlling the power absorption distribution from on-axis to off-axis.

3.2 High power measurement

A high power transmission measurement has been performed using the gyrotron in order to confirm the reliable operation and to measure the transmission efficiency. The beam power is measured with a calorimetric load at the gyrotron window, MOU output, and the waveguide mouth after transmission. The maximum power is 600 kW at the gyrotron output window under the condition of the beam voltage of 75 kV and the beam current of 24 A. The power loss rate at the MOU is about 16 %, and the transmission loss between the MOU exit and the waveguide mouth after transmission is 8 %. The transmission efficiency of corrugated waveguide, 92 % is estimated by the survey of over 20 shots at the conditions of the output power from 150 kW to 500 kW. The transmission loss may be caused by the misalignment of the waveguide at the MOU output including the offset and tilting, the ohmic consumption and the mode conversion. The loss at the barrier window is estimated less than 1 %. These results indicate that the system is performed reasonably as designed. The power injected to the Heliotron J vacuum vessel is up to 400 kW at the nominal gyrotron operation, 530 kW (beam voltage, V_B=75 kV, and beam current, I_B=21 A). Following the successful operation of the 70 GHz ECRH system, we have started the plasma experiment in Heliotron J. The current-free plasma can be produced at the second harmonic resonance condition, that is, the resonant magnetic field around 1.25 T.

4. Conclusion

We have designed and constructed the 70 GHz ECRH system for Heliotron J. The main objectives are to construct the system which can carry out the flexible experimental research on the heat and particle transport. The localization of the power absorption and the control capability of the injection angle and polarization enables us to perform a wide variety of plasma experiment.

We have tested the performance of the transmission components such as the waveguide in the low and high power measurement. The each component has a good performance as designed. The grooved mirror works as linear or circular polarizer depending on the groove depth. The launching system can focus the Gaussian beam well, and control the beam direction both toroidally and poloidally, which is a necessary condition in three dimensional confinement system as Heliotron J. This shows a wide control capability of the power absorption from on-axis to off-axis. We have started the plasma experiment using this 70 GHz ECRH system. The calculation of the power absorption profile under this ECRH launching condition is also underway by using a ray tracing code 'TRECE' [6]. The plasma experimental results will be shown in the forthcoming paper.

Acknowledgements

The authors would like to thank the Heliotron J group for operating the Heliotron J device.

References

[1] T. Obiki *et al.*, Nucl. Fusion, **41**, 833 (2001).
[2] J. A. Murphy, Int. J. Infrared Millimeter Waves **8**, 1165 (1987).
[3] K. Nagasaki *et al.*, Int. J. Infrared Millimeter Waves **20**, 823 (1999).
[4] A. Yariv, Quantum Electronics, Wiley, New York, 1967.
[5] L. Rebuffi *et al.*, Int. J. Infrared Millimeter Waves **10**, 291 (1989).
[6] V. Tribaldos *et al.*, Plasma Phys. Control. Fusion **40**, 2113 (1998).